Isolated spin 3/2 plaquettes in Na_3RuO_4

K.A. Regan[a,*], Q. Huang[b], R.J. Cava[a]

[a]*Department of Chemistry, Princeton University, Princeton, NJ 08544, USA*
[b]*NIST Center for Neutron Research, National Institute of Standards and Technology, Gaithersburg, MD 20899, USA*

Abstract

The crystal structure of Na_3RuO_4 determined by powder neutron diffraction is reported. The structure consists of isolated tetramers of edge sharing RuO_6 octahedra in the *ab* plane, creating isolated four-member plaquettes of Ru atoms comprised of two equilateral triangles sharing an edge. Magnetic susceptibility measurements reveal an antiferromagnetic transition at $\sim 29\,K$, with $\theta_w = -141\,K$. Neutron diffraction data indicate the onset of three-dimensional magnetic ordering at 29 K.
© 2005 Elsevier Inc. All rights reserved.

Keywords: Ruthenates; Na_3RuO_4; Magnetic properties.

1. Introduction

Ruthenates are rich in structure and varied in properties. Perovskite-based alkaline earth ruthenates ($MRuO_3$ or $M_{n+1}Ru_nO_{2n+1}$, where $M = $ Ca, Sr, Ba), exhibit properties varying from ferromagnetism in $SrRuO_3$ [1], to weakly temperature dependent Pauli paramagnetism in $BaRuO_3$ [2] to superconductivity in Sr_2RuO_4 [3]. Characterization of $Sr_3Ru_2O_7$ at higher temperatures point towards ferromagnetic interactions between the Ru atoms, while at lower temperatures, the compound crosses over to antiferromagnetic-like behavior [4] and becomes metamagnetic at high applied fields [5]. $CaRuO_3$ can be viewed in the same manner: its paramagnetic behavior can be tipped toward ferromagnetism by doping [6,7]. Such varied behavior of properties suggests that ruthenates sit on the boundary between magnetic and non-magnetic states.

The alkali metal ruthenates have not been as extensively studied. Recent work on the hollandites, KRu_4O_8 and $RbRu_4O_8$, revealed temperature independent Pauli paramagnetism [8] and metallic conductivity. Pauli paramag-

netism has also been observed in Li_2RuO_3 [9]. Although the magnetic properties of these three compounds are relatively ordinary, a further investigation of the alkali metal ruthenates may expose compounds that exhibit more unusual properties. For instance, Li_3RuO_4 exhibits short range antiferromagnetic ordering, with the possibility of spin freezing at $\sim 10\,K$ [10]. The Na–Ru–O system, for example, has not been thoroughly investigated, with several previously reported phases only superficially characterized [11]. Recently, Darriet et al. reported the structure and the magnetic properties of $NaRuO_2$ as well as Na_2RuO_4 [12,13]. $NaRuO_2$ displays paramagnetic behavior, while Na_2RuO_4 exhibits antiferromagnetic behavior attributed to short range ordering.

Although Na_3RuO_4 has been reported as being analogous in structure to Na_3NbO_4, the crystal structure was not previously refined, and magnetic data had only been collected from 77 to 600 K [14]. Mössbauer ^{99}Ru data were interpreted in terms of an antiferromagnetic long range ordering in Na_3RuO_4 at low temperature [15]. In this paper, we present the neutron diffraction refinement of Na_3RuO_4 and low temperature magnetic characterization. It is postulated that long range ordering of the spin 3/2 Ru^{5+} magnetic moments is frustrated by the isolated equilateral plaquettes present in the structure.

*Corresponding author. Fax: +609 258 6746.

E-mail address: kregan@princeton.edu (K.A. Regan).

2. Experimental

Polycrystalline samples of Na_3RuO_4 were synthesized using stoichiometric amounts of NaOH pellets (Merck, 97.0%) and RuO_2 powder (Alfa Aesar, Ru 54% min). The RuO_2 powder was heated prior to sample preparation at 700 °C for 2 h to remove any absorbed water. Reaction mixtures were placed in dense alumnia crucibles and heated first at 500 °C under flowing O_2 for 18 h and then at 650 °C under N_2 for 18 h, with an intermediate grinding.

Phase purity was determined via powder X-ray diffraction using Cu$K\alpha$ radiation. Resulting patterns corresponded with previously reported peak positions [14]. Magnetic characterization was performed using a Quantum Design PPMS magnetometer. The neutron powder diffraction intensity data of Na_3RuO_4 were collected at the NIST Center for Neutron Research, on a high resolution powder neutron diffractometer, with monochromatic neutrons of wavelength 1.5403 Å produced by a Cu(311) monochrometer. Collimators with horizontal divergences of 15′, 20′ and 7′ of arc were used before and after the monochromer and after the sample, respectively. Data were collected in the 2θ range of 3° and 168°, with a step size of 0.05′. The structural parameters were refined using the program GSAS [16]. The neutron scattering amplitudes used in the refinement were 0.363, 0.721, and 0.581 (10^{-12} cm) for Na, Ru and O, respectively. The magnetic peak intensity at $2\theta = 23.1°$ as a function of temperature for Na_3RuO_4 was measured with neutrons of wavelength 2.359 Å on the BT-2 triple-axis spectrometer at the NIST Center for Neutron Research, with a PG filter employed to suppress higher order wavelength contaminations.

3. Results

The structure of Na_3RuO_4 was refined to a monoclinic space group $C2/m$ (#12) with lattice parameters of $a = 11.0295(6)$ Å, $b = 12.8205(7)$ Å, $c = 5.7028(3)$ Å, and $\beta = 109.90(3)°$, and the initial atomic positions were taken as those of Na_3TaO_4 [14]. The neutron diffraction pattern is shown in Fig. 1. Atomic positions and thermal parameters are listed in Table 1: the final structure was very close to that of Na_3TaO_4. Relevant Ru–O and Na–O bond distances, as well as Ru–O bond angles, are listed in Tables 2 and 3, respectively. The average Ru–O bond length (= 2.01 Å) is similar to that reported for other Ru^{5+} compounds [17–19]. The oxygen coordination to the Ru atom creates two distinct octahedral environments (see Fig. 3). The octahedra are distorted both in bond lengths and bond angles. The distortions are similar to those seen in other ruthenates, such as β-La_3RuO_7 and $La_2Sr_2LiRuO_8$ [20,21]. In the present case, the irregular Ru–O bond lengths in the RuO_6
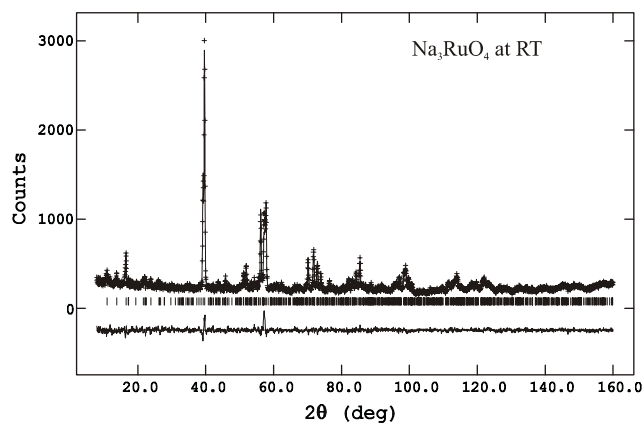

Fig. 1. Observed intensities (crosses) and calculated neutron diffraction pattern (solid line) Na_3RuO_4 at 295 K. Vertical lines show reflection positions. Differences between the observed and calculated intensities are shown at the bottom of the figure.

Table 1
Atomic positions and thermal parameters of Na_3RuO_4, e.g., $C2/m$ (#12) $a = 11.0295(6)$ Å, $b = 12.8205(7)$ Å, $c = 5.7028(3)$, $\beta = 109.908(3)$, $Z = 4$

Atom	Site	x	y	z	$U_{iso} \times 100\ (\text{Å}^2)$
Ru1	4g	0	0.1252(7)	0	0.59(11)
Ru2	4i	0.2550(9)	0	0.01777(16)	0.59(11)
Na1	4g	0	0.3759(15)	0	1.28(13)
Na2	4e	$\frac{1}{4}$	$\frac{1}{4}$	0	1.28(13)
Na3	8j	0.2421(13)	0.1254(10)	0.	1.28(13)
Na4	2c	0	0	1/2	1.28(13)
Na5	4h	0	0.2565(14)	1/2	1.28(13)
Na6	2d	0	$\frac{1}{2}$	1/2	1.28(13)
O1	4i	0.1147(14)	0	0.2019(27)	1.07(6)
O2	8j	0.1032(8)	0.2278(6)	0.2285(17)	1.07(6)
O3	4i	0.1528(12)	0	0.1969(23)	1.07(6)
O4	8j	0.1197(9)	0.1119(7)	0.8111(17)	1.07(6)
O5	8j	0.1455(8)	0.3924(7)	0.7636(16)	1.07(6)

$R_p = 5.38$, $R_w = 6.45$, $\chi^2 = 1.078$.
*Temperature parameters for Ru, Na and O were constrained to be equal, respectively.

octahedra result in equilateral Ru plaquettes, suggesting that Ru–Ru repulsion may play a role in the overall Ru–O geometry.

In a previous publication [14], the structure of Na_3MO_4 (M = Nb, Ru, and Ta) was viewed as a derivative of the NaCl structure with ordering of the NaO_6 and RuO_6 octahedra in planes parallel to the b-axis. However, from the magnetic point of view, it is advantageous to look at the structure with respect to the coordination and packing of the RuO_6 octahedra only, as it is the Ru that are responsible for the observed magnetic behavior. By doing so, the structure of Na_3RuO_4 can be viewed as consisting of isolated tetramers of edge-sharing RuO_6 that lie in the ab plane. The planes of RuO_6 octahedra are separated by a layer
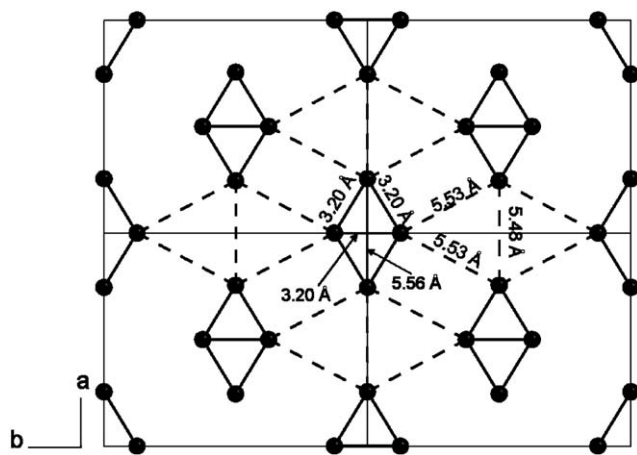
Table 2
Bond lengths and bond angles in Na_3RuO_4

	Bond length (Å)		Bond length (Å)
Ru1–O1 2	2.124(12)	Na3–O1	2.485(17)
Ru1–O2 2	1.927(11)	Na3–O2 2	2.270(16)
Ru1–O4 2	1.976(9)	Na3–O3	2.280(16)
		Na3–O4	2.455(16)
Ru2–O1	2.146(14)	Na3–O5	2.382(15)
Ru2–O3	1.839(13)		
Ru2–O4 2	2.115(11)	Na4–O1 2	2.440(13)
Ru2–O5 2	1.931(11)	Na4–O4 4	2.314(9)
Na1–O2 2	2.365(18)	Na5–O2 2	2.243(8)
Na1–O3 2	2.312(14)	Na5–O4 2	2.596(15)
Na1–O5 2	2.431(8)	Na5–O5 2	2.495(15)
Na2–O2 2	2.416(7)	Na6–O3 2	2.795(11)
Na2–O4 2	2.303(9)	Na6–O5 4	2.257(8)
Na2–O5 2	2.328(8)		

Table 3
O–Ru–O and Ru–O–Ru bond angles within the tetramers of Na_3RuO_4

	Bond angle (deg)		Bond angle (deg)
O1–Ru1–O1	81.8(7)	O1–Ru2–O3	168.6(7)
O1–Ru1–O2	92.5(4)	O1–Ru2–O4	77.5(4)
O1–Ru1–O2	171.1(4)	O1–Ru2–O5	91.7(5)
O1–Ru1–O4	81.1(5)	O3–Ru2–O4	94.2(5)
O1–Ru1–O4	91.4(5)	O3–Ru2–O5	96.2(5)
O2–Ru1–O2	94.0(7)	O4–Ru2–O4	85.4(6)
O2–Ru1–O4	94.4(4)	O4–Ru2–O5	90.7(4)
O4–Ru1–O4	170.1(7)	O4–Ru2–O5	169.1(6)
		O5–Ru2–O5	91.2(7)
Ru1–O1–Ru1	98.2(7)		
Ru1–O1–Ru2	95.5(5)		
Ru1–O4–Ru2	97.5(5)		

Fig. 2. Crystal structure of Na_3RuO_4, represented as two unit cells in the c-direction. Na atoms are shown in light grey. The Ru (dark spheres) are in octahedral coordination with oxygen. The RuO_6 units are shown as grey octahedra.

Fig. 3. Ru–O arrangement in the tetramer created by edge sharing of 4 RuO_6 octahedra in Na_3RuO_4. The two types of Ru atoms are shown as large black spheres (Ru1) and large light gray spheres (Ru2), respectively, and the oxygens are small gray spheres. The Ru–Ru connectivity is added to emphasize the equilateral triangular arrangement of the Ru atoms.

of Na atoms (Fig. 2). An individual tetramer is shown in Fig. 3.

The edge sharing motif of the four RuO_6 octahedra creates Ru plaquettes comprised of two edge-shared equilateral triangles of Ru atoms. Fig. 4 represents the structure in the ab plane, with only the Ru atoms shown. The isolated four-member plaquettes are clearly visible. The distance between neighboring Ru atoms in the plaquettes is 3.20 Å, and the equilateral triangles are apparent in the figure. The four-membered plaquettes are then arranged in a centered arrangement in the ab plane. The vertices of the plaquettes connect to form larger plaquettes of nearly equilateral triangles, with Ru–Ru distances of ~5.5 Å. The layer shown in Fig. 4 repeats by stacking along the c-axis, with the 119° β angle indicating that the plaquettes are not stacked directly over one another. The distance to the next plane along c is 5.7 Å. The Ru within the triangle-based plaquettes are spaced at 3.2 Å, with a frustrated triangular geometry to the nearest neighbor plaquettes

at a much larger distance, 5.5 Å or more. This indicates that the coupling between neighboring plaquettes will be much weaker than the coupling within a plaquette, and may in fact also be frustrated.

Measurement of the magnetic susceptibility from 5 to 250 K (Fig. 5, inset A) reveals Curie–Weiss behavior, with an antiferromagnetic-like ordering transition at low temperature ($T_{trans} \sim 29$ K). The transition lacks the cusp-like character typically observed in three-dimensional antiferromagnetic ordering transitions. Linear fitting of the high temperature data of the inverse

Fig. 4. Structure of Na_3RuO_4 in the *ab* plane showing the Ru atoms only (4 unit cells). The isolated plaquettes of Ru atoms are shown by bold lines. The distances within the plaquette, 3.2 Å, are much shorter than the distances to the next plaquette. The triangular distribution of neighboring plaquettes is shown by dashed lines.
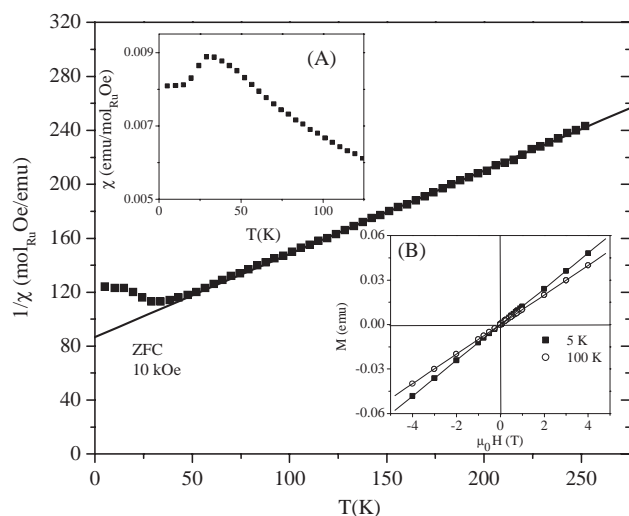

Fig. 5. Inverse magnetic susceptibility $(1/\chi)$ vs. *T* of Na_3RuO_4 with an applied DC field of 10 kOe. A linear fit of the high temperature data (100–250 K) shows Curie–Weiss behavior. Inset A: The antiferromagnetic-like transition observed in Na_3RuO_4. Inset B: The *M* vs. *H* (0–5 T) loops at 5 and 100 K show linear behavior.

susceptibility from 100 to 250 K (Fig. 5) allowed for the determination of θ_w and μ_{eff}. The observed value for μ_{eff} is 3.60 μ_B. This is similar to the value expected for the spin only moment of an $S = 3/2$ ion (3.87 μ_B), which is what is expected for $4d^3$ Ru^{5+}. The θ_w value was determined to be −141 K. However, temperatures much lower than θ_w are needed for the magnetic transition to occur: Na_3RuO_4 displays an observed θ_w/T_N ratio of approximately 5/1. *M* vs. *H* loops reveal linear behavior at 5 and 100 K, as would expected for the antiferromagnetically aligned Ru moments. No ferromagnetic component is observed (Fig. 5, inset B). The $1/\chi$ data begin to deviate from the high temperature Curie–Weiss

law at ~55 K, suggesting the presence of antiferromagnetic fluctuations approximately 25 K above the ordering temperature.

Neutron diffraction data were collected at 3.5 and 48 K on the BT2 diffractometer at NIST. Fig. 6 shows the difference between the diffracted intensity at 3.5 and 48 K. The data show the presence of magnetic ordering at low temperatures, with peaks at 21.9° and 23.1°. The magnetic peak width is that of the instrumental resolution, indicating the ordering is three-dimensional in character. Further, the scattering occurs at positions that not associated with Bragg peaks, verifying that the ordering is antiferromagnetic in character. Fig. 7 plots the intensity of the strongest magnetic scattering ($2\theta = 23.1°$) as a function of temperature, on both heating and cooling. The onset of the 3-D ordering occurs at the same temperature as the main feature in the magnetic susceptibility data. The neutron diffraction data are consistent with the analysis of Mossbaüer effect data on the compound taken by Gibb et al. [15].
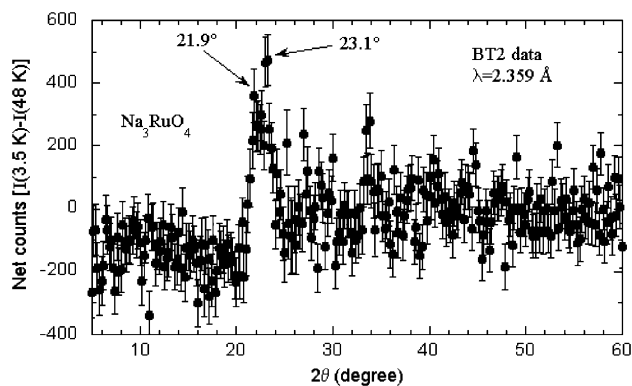

Fig. 6. Difference between the 3.5 and 48 K of the low angle neutron powder diffraction pattern of Na_3RuO_4, in the region in which the strongest magnetic ordering peaks are expected to occur. Magnetic scattering peaks are observed at 21.9° and 23.1°, indicting the presence of magnetic ordering. The position of the peaks (off Bragg peaks) is indicative of antiferromagnetic ordering.
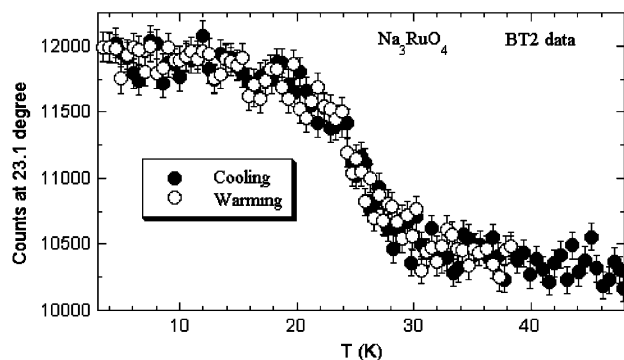

Fig. 7. Temperature dependence of magnetic scattering intensity at 23.1° upon warming and cooling. The onset of magnetic ordering at ~30 K corresponds to the ordering temperature observed in the magnetic susceptibility data.

4. Conclusions

We have reported the structure of Na_3RuO_4, determined via powder neutron diffraction. This layered structure is comprised of tetramers of RuO_6 octahedra, resulting in two equilateral triangles of Ru atoms sharing a single edge to form isolated equilateral plaquettes. Magnetic susceptibility measurements reveal antiferromagnetic ordering of spin 3/2 moments at $T_c \sim 29\,K$, approximately a factor of five below θ_w, determined to be $-141\,K$. Although such a ratio cannot be considered to be indicative of strong geometric frustration [22], it is possible that the triangular geometry of the Ru atoms supresses long range ordering observed by neutron diffraction to lower temperatures. We are not aware of theoretical models of systems of isolated plaquettes of this type, and both theoretical modeling and further characterization of the magnetic transition may be of interest.

Acknowledgments

References

[1] A. Callaghan, C.W. Moeller, R. Ward, Inorg. Chem. 5 (1966) 1572.

[2] J.T. Rijssenbeek, R. Jin, Y. Zadorozhny, Y. Liu, B. Batlogg, R.J. Cava, Phys. Rev. B 59 (1999) 4561.

[3] Y. Maeno, H. Hashimoto, K. Yoshida, S. Nishizaki, T. Fujita, J.G. Bernorz, F. Lichtenberg, Nature 372 (1994) 532.

[4] R.J. Cava, J. Chem. Soc. Dalton Trans. 19 (2004) 2979.

[5] R.S. Perry, L.M. Galvin, S.A. Grigera, L. Capogna, A.J. Schofield, A.P. Mackenzie, M. Chiao, S.R. Julian, S.I. Ikeda, S. Nakatsuji, Y. Maeno, C. Pfleiderer, Phys. Rev. Lett. 86 (2001) 2661.

[6] T. He, R.J. Cava, Phys. Rev. B 63 (2001) Art. No. 172,403.

[7] T. He, R.J. Cava, J. Phys.: Condens. Matter 13 (2001) 8347.

[8] M.L. Foo, W.L. Lee, T. Siegrist, G. Lawes, A.P. Ramirez, N.P. Ong, R.J. Cava, Mater. Res. Bull. 39 (2004) 1663.

[9] I. Felner, I.M. Bradaric, Physica B 311 (2002) 195.

[10] A. Alexander, P.D. Battle, J.C. Burley, D.J. Gallon, C.P. Grey, S.H. Kim, J. Mater. Chem. 13 (2003) 2612.

[11] I.S. Shaplygin, V.B. Lazarev, Russ. J. Inorg. Chem. 25 (1980) 1837.

[12] M. Shikano, C. Delmas, J. Darriet, Inorg. Chem. 43 (2004) 1214.

[13] M. Shikano, R.K. Kremer, M. Ahrens, H.-J. Koo, M.-H. Whangbo, J. Darriet, Inorg. Chem. 43 (2004) 5.

[14] J. Darriet, J. Galy, Bull. Soc. fr. Minéral. Cristallogr. 97 (1974) 3.

[15] T.C. Gibb, R. Greatrex, N.N. Greenwood, J. Solid State Chem. 31 (1980) 153.

[16] A. Larson, R.B. Von Dreele, Los Alamos National Laboratory, Internal Report, 1994.

[17] J. Darriet, F. Grasset, P.D. Battle, Mater. Res. Bull. 32 (1997) 139.

[18] W.R. Gemmill, M.D. Smith, H.C. zur Loye, J. Solid State 177 (2004) 3560.

[19] E. Quarez, F. Abraham, O. Mentre, J. Solid State 176 (2003) 137.

[20] P. Khalifah, D.M. Ho, Q. Huang, R.J. Cava, J. Solid State 165 (2002) 359.

[21] J.A. Rodgers, P.D. Battle, N. Dupré, C.P. Grey, Sloan, J. Chem. Mater. 16 (2004) 4257.

[22] A.P. Ramirez, Annu. Rev. Mater. Sci. 24 (1994) 453.